IMPACT OF THERMAL AGING ON CRACK GROWTH BEHAVIOR OF LEAD FREE SOLDER INTERCONNECTS

by

ANURAAG KARNIK

Presented to the Faculty of the Graduate School of

The University of Texas at Arlington in Partial Fulfillment

of the Requirements

for the Degree of

MASTER OF SCIENCE IN MECHANICAL ENGINEERING

THE UNIVERSITY OF TEXAS AT ARLINGTON

MAY 2018

Acknowledgements

I would like to use this opportunity to express my gratitude to Dr. Dereje Agonafer for giving me a chance to work at EMNSPC and for his continuous guidance during that time. It has been a wonderful journey working with him in research projects and an experience to learn so much from the several conference visits. I also thank him for serving as the committee chairman.

I would like to thank Dr. A. Haji-Sheikh and Dr. Fahad Mirza for serving on my committee and providing numerous learning opportunities.

Furthermore, I am grateful to the entire EMNSPC team. Special thanks to Pavan Rajmane and Madhuri Karnik for helping me throughout my master's thesis.

May 03, 2018

Abstract

IMPACT OF THERMAL AGING ON RELIABILTY ASSESSMENT OF CRACK GROWTH BEHAVIOR IN LEAD FREE SOLDER INTERCONNECTS.

Anuraag Karnik, MS

The University of Texas at Arlington, 2018

Supervising Professor: Dereje Agonafer

Reliability assessment helps in better performance of electronic packages. This also helps electronic device manufacturing company as well as the users to evaluate the life of any device. The microstructure, mechanical response, and failure behavior of Pb-free solder joints in electronic assemblies are constantly evolving when exposed to isothermal aging and/or thermal cycling environments. Due to reflow process or exposure to harsh environment conditions, packages are subject to fatigue loads which can accelerate crack growth in the solder interconnects. But, some material after aging get hardened and decrease in plastic deformation capacity. This effect sometimes leads to better crack resistance due to surface roughness. A direct and detrimental effect on packaging reliability is observed during elevated temperature thermal aging for Pb-free BGA packages. In past studies, researchers have revealed that pb-free material undergo significant change in mechanical properties and which in turn influences stress-strain behavior of solder. The stresses developed due to CTE mismatch of different materials used in package causes failure of the solder interconnects.

In this thesis, an attempt has been made to study damage progression of cracks that occurs in solder interconnects and its relation to Stress Intensity Factor (SIF) for different thermal aging and thermal cyclin profiles. Experimental test was performed for

different temperatures and time on the solder and PCB. Dynamic mechanical analysis (DMA) and thermomechanical analysis (TMA) are used for characterizing thermomechanical properties of the solder and PCB material. A finite element model and theory associated with experimental observations has been employed for understanding fracture of solder interconnects due to aging of solder and PCB. Also, FEA has been made use of to calculate all stress components and its variations through time and along the area of interest i.e. circumferential area of solder ball interconnects, up to 25μm along the length of the interconnects. Failure progression is analyzed by creating a relation between crack dimensions, stress developed and load. The analysis leads to better understanding of crack propagation, evaluating relation between thermal load, stress intensity factor, crack dimension and reduces experimenting time and cost.

Table of Contents

List of Illustrations

List of Tables

Chapter 1

INTRODUCTION

1.1 Electronic Packaging

Cluff, K.D. et. Al in “Mechanical Engineering Handbook” define electronic packaging as the art and science of connecting circuitry to reliably perform some desired function in some application environment. It is a multi-disciplinary subject which needs knowledge of all field i.e. Mechanical, Industrial and Electrical Engineering, Chemistry, Physics and Material Science Department. The most prominent areas to work are heat transfer, material science, electrical and mechanical stability and manufacturing. These packages include different electrical components like transistors, capacitors, resistors, diodes which in turn must be interconnected to perform a specific task.

Therefore, an electronic package must serve some essential functions:

A. Signal Distribution

B. Heat Dissipation

C. Power Distribution

D. Mechanical Support, chemical, electromagnetic and environmental protection.

Figure 1-1shows hierarchy of interconnection levels and details explained below:

Level 0

- Gate-to-gate interconnections on the silicon die

Level 1

- Connections from the chip to its package

Level 2

- PCB, from component to component or to external connector

Level 3

- Connections between PCBs, including backplanes or motherboards

Level 4

- Connections between subassemblies, for example a rack

Level 5

- Connections between physically separate systems, using for example an Ethernet LAN

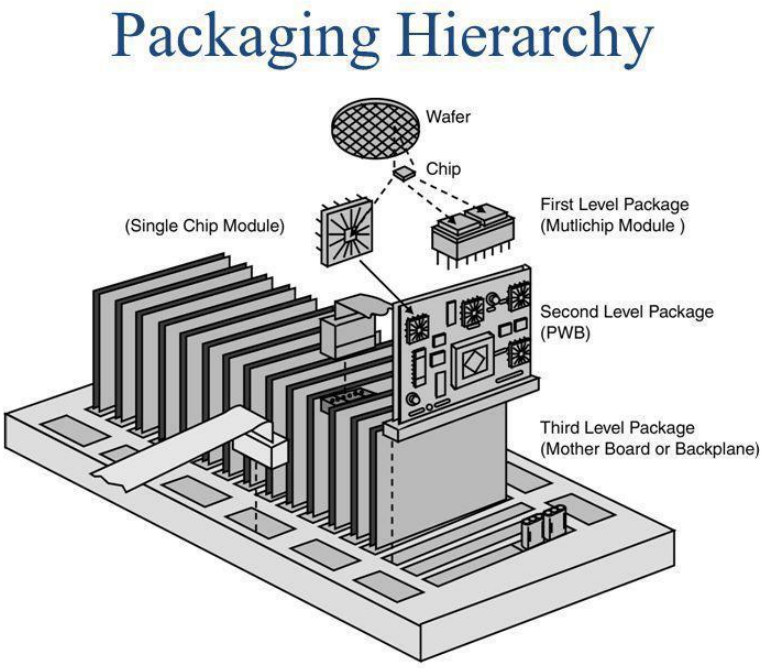

Figure 1-1 Hierarchy of Interconnection Levels

1.2 Package Classification

Packages can be broadly classified as-

- Through Hole Mount IC Packages

- Dual in-line Package(DIP)
- Pin Grid

- Surface Mount IC Packages

- Quad Flat Package(QFP)
- Thin small outline package(TSOP)
- Small outline J-leaded package (SOJ)
- Ball Grid Array (BGA)

- Chip Scale IC Packages

- Chip Scale Package (CSP)
- Wafer Level
- Stacked Die (2.5D & 3D Packages)

Initially Semiconductor industry used Through hole technology to mount package on board in which pins of the component go through the previously drilled holes in PCB. In this kind of packaging signal had to pass through all PCB layers and due to low density one sided mounting was available. To fill the gap Surface Mount Technology (SMT) was invented which allowed pins of the device to directly mount on the surface of PCB. Provided much higher density and can be mounted at both sides of PCB. On the other hand, Chip Scale Package, or CSP, based on IPC/JEDEC J-STD-012 definition, is a single-die, direct surface mountable package with an area of no more than 1.2 times the original die area. CSP is an evolution of SMT in which passive components such as resistors, capacitors must also be miniaturized to further improve the speed performance. These packages are hardly serviceable due to difficult fabrication process and there are issues related to long term reliability which need to be taken care of. Figure 1-2 shows below shows the progress of packaging technology over the years.

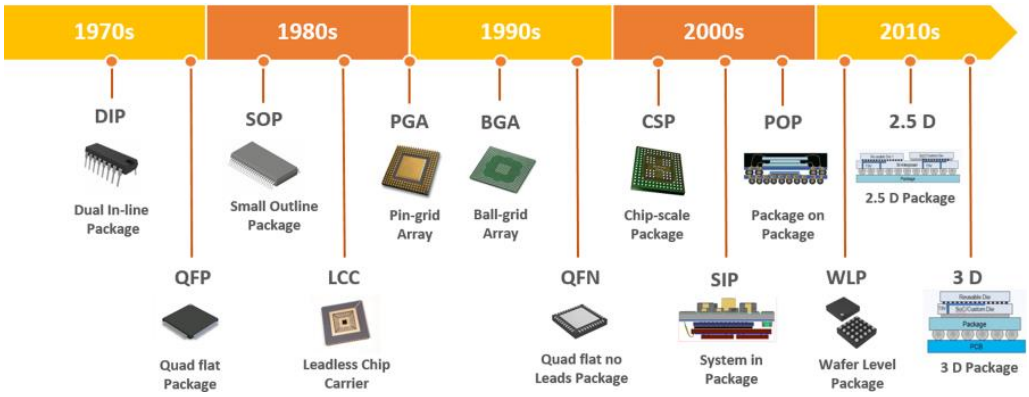

Figure 1-2 Progress of Packaging Technology

1.3 BGA Package

In Ball grid array(BGA) solder ball which are used to interconnect the printed circuit board(PCB) and integrated circuit(ICs) are arranged in grid pattern. The copper pads on PCB allows conduction of electric signal from ICs to PCB through solder balls. Instead of perimeter, In BGA whole bottom surface of ICs used for the solder ball interconnections also called as area array package. For the assembly of solder ball, ICs along with BGA solder balls place on top of PCB. Heat generated by reflow over or infrared heater used to melt solder balls, and surface tension helps to hold the package in alignment with solder ball.

BGA packages are available in various types:

- HSBGA – BGA with heat spreader
- FCBGA – flip chip BGA
- CSBGA – cost saving BGA
- FCHSBGA – flip chip BGA with heat spreader

- FBGA: fine pitch ball grid array, with a square or rectangular array of solder balls on one surface
- LBGA: Low Profile Ball Grid Array
- TEPBGA: Thermally Enhanced Plastic BGA
- CBGA: Ceramic Ball Grid Array
- OBGA: Organic Ball Grid Array
- TFBGA – thin fine pitch BGA.
- PBGA: Plastic Ball Grid Array
- μBGA – micro-BGA, with ball spacing less than 1 mm
- LFBGA – low profile fine pitch ball grid array
- TBGA: Thin Ball Grid Array

Advantages of BGA packages are as follows:

- It is used in Microcontrollers, Microprocessors, RAM devices, PC Chipsets etc.
- It has lower inductance power planes which support high frequency designs.
- It supports higher pin counts compare to wire bond packages.
- It has improved current distribution which minimizes IR drops. In BGA, power is distributed through top metal layer metal bumps.
- It has Excellent thermal compatibility with PCB.
- Auto registration capability and low cost.
- PBGA type supports excellent electrical performance.
- CBGA and TBGA support better heat dissipation compare to PBGA type.

Disadvantages of BGA packages are as follows:

- Solder balls cannot flex in the way longer leads can. (non- compliant)
- Once the package is soldered into place, it is difficult to find soldering faults.
- During development it is not practical to solder BGAs into place, and sockets are used instead, but tend to be unreliable.
- Expensive equipment is required to reliably solder BGA packages; hand-soldering BGA packages is very difficult and unreliable.

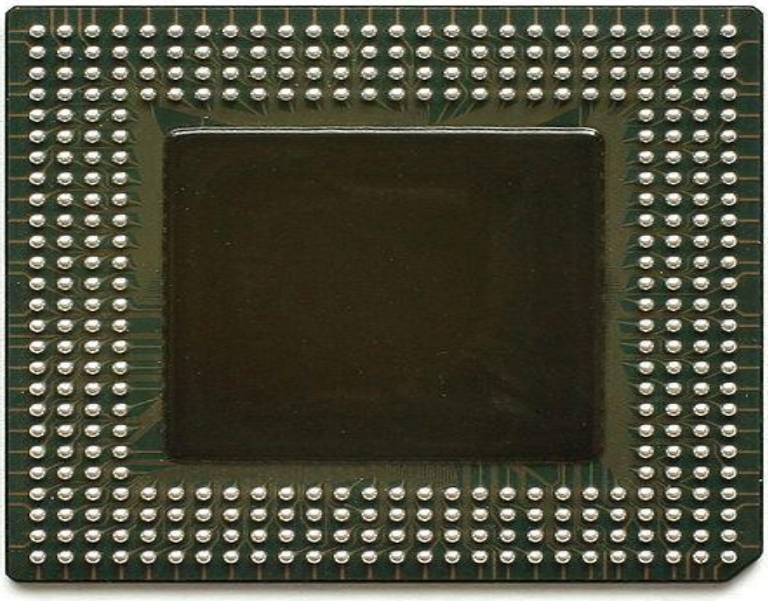

Figure 1-3 Ball Grid Array Package

1.3.1 Reliability issues with solder interconnects

With advancements in technology the packages have become smaller which in turn have led to high density packages meaning smaller solder balls and smaller distance between the solder balls. Smaller solder interconnects are generally impacted more by the thickness and morphology of intermetallic compounds (IMCs) and composition of the bulk solder alloy than larger solder interconnects. The microstructure mechanical response, and failure behavior of lead-free solder joints continually evolve during isothermal aging and/or thermal cycling environments. Furthermore, it has also been seen that microstructure and mechanical behavior can change significantly for SAC solders due to thermal aging. Also, significant cycle lifetime degradation or up gradation has been previously observed for various solder alloys depending on aging time and temperature. Ultimately because of thermal aging and thermal cycling cracks are developed on the solder interconnects.

1.4 Motivation

To tackle the above-mentioned reliability issue, rising due to effects of IMC growth and composition of bulk solder alloy, there is a need to understand the crack growth behavior under thermo mechanical loading. The region on lead free solder interconnects is most susceptible to failure and consequently techniques to find out critical cracks must be proposed. SAC solders are now predominant and therefore this study is done taking SAC solders in consideration as these types of solders are used in every product manufactured having electronic packages.

1.5 OBJECTIVE AND SCOPE

In this study experimental as well as finite element technique has been made use of to examine the critical crack in the solder interconnects after the package has been exposed to thermal aging and subsequently to thermal cycling. A multi-level finite element (MLFE) (sub modeling) technique has been leveraged to carry out whole analysis in ANSYS WORKBENCH 18.0. Crack propagation in the solder interconnects is analyzed under the loading condition of thermal cycling (JESD22-A104D). J-integral and Stress Intensity Factor (SIF) obtained from the FE analysis is utilized to identify the critical crack and its mode of failure. In addition, effects of cracks and thermal on the plastic work and cycles to failure of package have been found out.

CHAPTER 2

LITERATURE REVIEW

Zhang et al. [1] studied the effects of thermal aging on thermal cycling reliability of lead free fine pitch packages. They concluded that isothermal aging and/or thermal cycling had significant cycle lifetime degradation for both SAC 305 and SAC 405. Failure analysis showed significant bulk Ag_3Sn coarsening and intermetallic Cu6Sn5 growth at the solder joint interfaces.

Motalab et al. [2] in their research studied the effects of aging on the nine Anand model parameters by performing stress strain tests on SAC 305 samples that were aged using isothermal aging for various temperature and times. The revised Anand's constitutive equation with evolving parameters were then implemented in commercial FEA codes. In addition, new aging aware failure criteria have been developed based on fatigue data for lead free solder uniaxial specimens that were aged at elevated temperature for various durations prior to mechanical cycling. Using the measured fatigue data, mathematical expressions have been developed for the evolution of the solder fatigue failure criterion constants with aging.

Xu et al. [3] studied the effects of thermal aging and thermal cycling on the growth of IMCs between Pb-free and Pb-based solders. They concluded e growth rate of the IMC layer can affect the solder joint reliability. Furthermore, an integration model suggesting non-aging thermal cycling and aged thermal cycling was recommended to predict the IMC growth for different thermal cycling aging profiles and is most significant for long-period thermal cycling profiles.

Yang and Cui [4] presented in their research effects of thermal aging the mechanical properties of molding compounds and reliability of electronic packages. They also presented an experimental study of the same by using Dynamic Mechanical Analyzer

(DMA) and Thermo-mechanical Analyzer (TMA) to measure the moduli, coefficients of thermal expansion (CTE), and the glass transition temperature (Tg). A numerical model was then used to estimate the modulus of the oxidized layer. 3D finite element models were established to simulate the impact of the aging effect on the stress/strain of the package. The modeling results indicate that the aging of the compounds have a significant impact on the stress/strain status in the package.

Rodgers et al. [5] studied the FE modelling of a BGA package subjected to thermal and power cycling. They used sub structuring and submodelling techniques to estimate the fatigue life of the solder joints under various thermal loading conditions. They showed that submodelling technique includes three stages. First, a coarsely meshed model is analyzed, and regions of interest are identified. Second, a portion of the coarse model around the region of interest is extracted and meshed with a much higher density of elements. The degrees of freedom of the nodes along the “cut” boundary is then interpolated from the coarse model results. In addition, all nodal temperatures are interpolated from the coarse model. Finally, the sub model is analyzed, and results interpreted. Furthermore, they suggested that care should be taken to ensure that the stress distribution along the cut boundary is comparable with the coarse model (St Venant’s principle).

Wang et al [11] performed a finite element analysis and leveraged sub modelling. He modelled a bimetallic strip of two commonly used electronic packaging materials such as silicon and eutectic solder alloy. They then compared the results from the simplified global geometry with the results from detailed sub model geometry under fatigue loading. Results for sub modelling case were found to be more accurate.

J.H. Lau [6] investigated thermal fatigue behavior of solder joints by nonlinear finite element (FE), Coffin-Manson, and fracture mechanics methods. In the fracture mechanics method, a total of seven different crack lengths were studied and ΔJ has been calculated at three

contours around the crack tip. The best fit equations for the average values of ΔJ is used. It was concluded that there was very large stress around the crack tip. This stress however, becomes much smaller as soon as it is away from the crack tip. As a matter of fact, except near the crack tip, the stresses in the cracked solder joints are smaller than those in the uncracked solder joint.

Raju and Newman Jr. [7] in their research of stress intensity factors for a wide range of semi-elliptical cracks in finite thickness plates presented stress-intensity factors for shallow and deep semi-elliptical surface cracks in plates subjected to uniform tension using finite element method. The finite-element analysis gave stress-intensity factors along the crack front generally within 1% of the exact solution, except in the region of sharpest curvature of the ellipse, where the calculated values were about 3% higher than the exact solution. Further refinement in the mesh size in this area gave more accurate stress-intensity factors. Because the present method yielded stress-intensity factors for completely embedded semi elliptical cracks generally within 0.4-1% of the exact solutions, the method was considered suitable for analyses of more complex configurations, provided that enough degrees of freedom were used to obtain good convergence.

Begley and Landed [8] studied J-integral as a fracture criterion. They suggested that the path independent J integral, as formulated by Rice, can be viewed as a parameter which is an average measure of the crack tip elastic-plastic field. This together with the fact that J can be evaluated experimentally, makes a critical J value an attractive elastic-plastic fracture criterion. The J_{ic} fracture criterion refers to crack initiation under plane strain conditions from essentially elastic to fully plastic behavior Experiments supporting the validity of a J_{ic} fracture criterion were presented in their paper. Furthermore, they suggested that the J integral is an average measure of the near tip stress strain environment of cracked elastic plastic bodies, as such it is an attractive failure criterion and being a field

parameter J-integral is compatible with crack opening dislocations and other approaches concerned with specific crack tip features.

Rahangdale et al. [9] studied the failure progression in a 3D TSV package by creating a relation between crack dimension, the stress developed, and load applied. The analysis helped in better understanding of crack propagation and evaluating the relation between thermal load, stress intensity factor and crack dimensions. The relation between crack location and K1, K2, K3 was obtained. Also, the relation between J-Integral, the length of the crack, die thickness and crack size has been calculated. Furthermore, ANSYS 17.2 bundles are used for modeling and simulation and finite element analysis (FEM) is used to calculate stress intensity factor (SIF) at the crack interface.

Yu et al. [10] in their research of dynamic behavior of electronic package and impact reliability of BGA solder joints studied the crack growth assessment in drop impact problem. From the findings it was inferred that the behavior of the crack growth can be evaluated by elastic fracture mechanics theory. The elastic FEA was carried out to calculate the stress intensity factor K, where only K, was adjusted because the mode I deformation was dominant. Furthermore, it was found that based upon the repetitive drop tests, i relation between the fatigue life and the falling height can be divided into two domains. If the falling height is higher than a critical value, an unstable fracture of interface crack will occur, and the dynamic fracture toughness for the interface crack in a solder joint can be roughly established at K_{IC}=15MPa*$m^{0.5}$.

CHAPTER 3

MATERIAL CHARACTERIZATION

Material characterization refers to the broad and general process by which a material's structure and properties are probed and measured. "Characterization describes those features of the composition and structure (including defects) of a material that are significant for a particular preparation, study of properties, or use, and suffice for the reproduction of the material. In this study the work is limited to determine properties of material. To predict more accurate results through ANSYS workbench, it is necessary to provide more accurate inputs. To characterize the material following parameters were considered:

- Coefficient of Thermal Expansion (CTE)
- Young' Modulus (E)
- Poisson's Ratio (υ)

To determine these properties the equipment and techniques used are given below:

- Sun Microsystems Temperature Chamber
- Thermo-mechanical Analyzer (TMA) – Hitachi TMA 7000
- Dynamic Mechanical Analyzer (DMA) – Hitachi DMA 7100

Sample preparation and test procedures for all the tests conducted for material characterization will be explained in this section.

3.1 Thermo-mechanical Analyzer

3.1.1 CTE

Coefficient of Thermal Expansion (CTE) is defined as the tendency of a material which defines the extent to which a material expands upon heating. CTE may also be defined as the fractional change in length or volume of a material for a unit change in temperature.

$$\alpha = \epsilon / \Delta T$$

Where,

α – Coefficient of Thermal Expansion (CTE) ppm/°C

ϵ - Strain (mm/mm)

ΔT – Difference in Temperature (°C)

3.1.2 Glass Transition Temperature (T_g)

The Glass Transition Temperature (Tg) is one of the most important properties of any polymer where the polymer transitions from a hard, glassy material to a soft, rubbery material. Tg is not a discrete thermodynamic transition, but a temperature range over which the mobility of the polymer chains increases significantly. The Tg of a polymer depends on the chemical structure of the resin, type of hardener and the degree of cure.

TMA consist of a quartz probe whose relative movement with change in temperature is used as a parameter to determine the CTE of the PCB material. The quartz probe is enclosed in a thermal chamber which can be operated in a wide range of temperatures. Temperatures as low as -650C can be achieved using a cooling attachment. The TMA with the cooling attachment is shown in the figure 3.1. PCB samples for the TMA with dimensions 8mm X 8mm are cut using a high-speed cutter. The TMA samples are shown in the figure 3.2. The TMA samples are subjected to a temperature range of -650C to

2600C with a ramp rate of 50C/min. The start and end load applied is 100mN. The in-plane and out of plane CTE are measured using the TMA by changing the position of the PCB sample.

Figure 3-1 TMA 7000

Figure 3-2 and 3-3 shows the plot for CTE of Solder and PCB. The plots have been made over a range of 0 to 100 deg C. Further experiments for PCB showed a significant change in slope is observed in the plots after 150^0C which is due to the recrystallization and cold crystallization of the samples during the experiment. The glass transition range of the samples is the region where the change of slope in the CTE plots is observed. Further expansion of the sample is observed above 180^0C and the melting process takes place at about 2250C with the reduction in sample dimensions and viscosity. As for solder it was seen CTE for no aging > 80 deg > 125 deg.

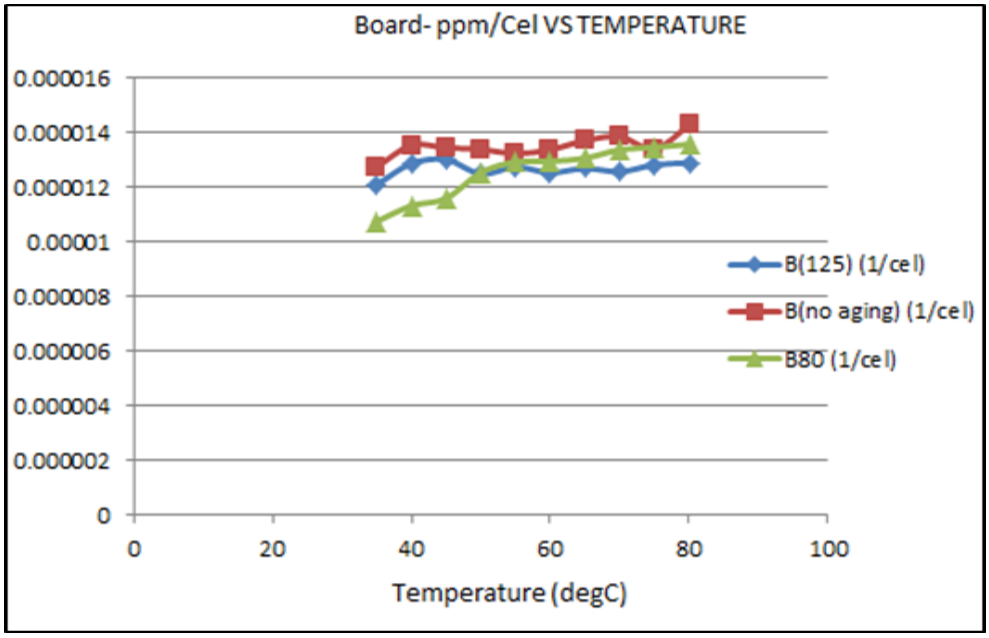

Figure 3-2 CTE Results For PCB

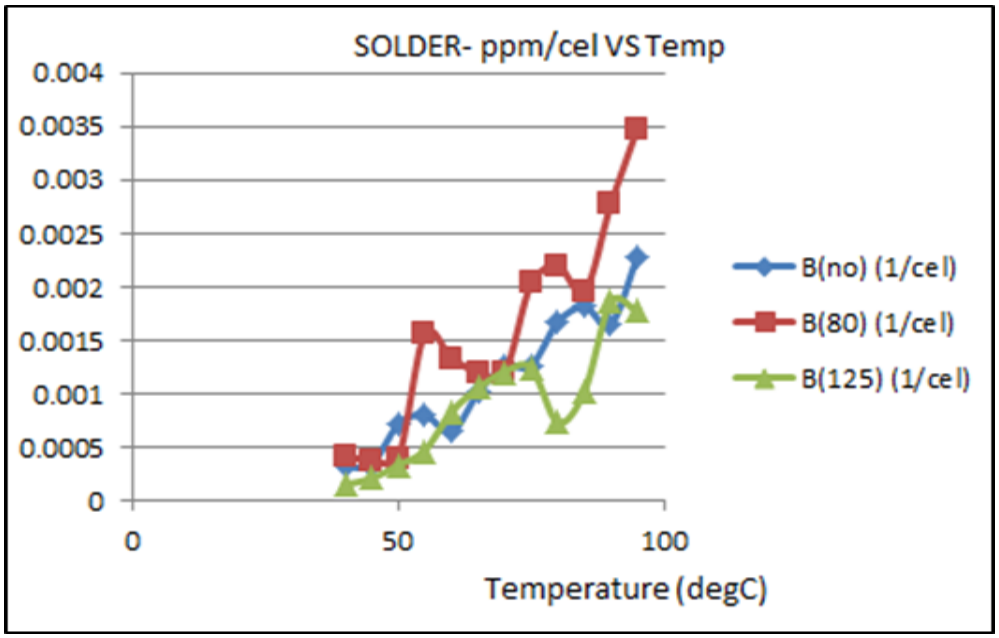

Figure 3-3 CTE Results for Solder

Material	CTE (ppm/ºC)
Copper Pad	17.78
Die Attach	65
Die	2.94
Mold	8.43
Polyimide Layer	35
Solder Mask	30

Table 3-1 CTE of Components

Material	CTE No aging	CTE aging 80	CTE aging 125
Board	1.34773E-05	1.26542E-05	1.25378E-05
Solder	0.001525735	0.001579035	0.001773808

Table 3-2 CTE average from the plots

3.2 Dynamic-Mechanical Analyzer

3.2.1 Storage Moduli (E')

The storage modulus is the measure of energy stored, representing the elastic portion of a material. Materials that deform by a small amount when tensile load is applied to them are said to be stiffer as compared to the materials that deform by a considerable amount when tensile or compressive loading is applied to them. Mathematically, Young's Modulus is defined by the stress produced in a material when some strain is applied to it.

$$E = \sigma / \varepsilon$$

Where,

E – Young's Modulus (MPa)

σ – Stress (MPa)

ϵ - Strain (mm/mm)

3.2.2 Loss Moduli (E'')

The Loss Modulus is the measure of energy dissipated as heat, representing the viscous portion of the material.

3.2.3 Complex Modulus (E_c)

The complex modulus is a complex number whose real part is storage modulus (E') and the imaginary part is the loss modulus (E'').

$$E_c=(E') + i(E'')$$

3.2.4 Young's Modulus (E)

Young's modulus is the elastic modulus used to calculate the deformation of a material which takes place when a force parallel to the axis of the object is applied to one face which the opposite face is held fixed by another equal force. It is also called as Tensile Modulus or Modulus of Elasticity or Elastic Modulus. It is a measure of stiffness of the PCB. The argument of the complex modulus (Ec) is the measure of the Young's Modulus (E).

$$|Ec| = E = [(E')^2 + (E'')^2]^{1/2}$$

The Dynamic Mechanical Analyzer (DMA) is used to measure the complex modulus (Ec), using which the Young's modulus (E) of the PCB material is calculated. The PCB sample of dimensions 50mm X 10mm in length and width, is clamped in a bending apparatus. Care should be taken that the sample is doesn't gets displaced during the experiment. A sinusoidal wave is generated using a force motor which transmits it to the sample through a drive shaft. This applies a cyclic load due to which the sample is deformed.

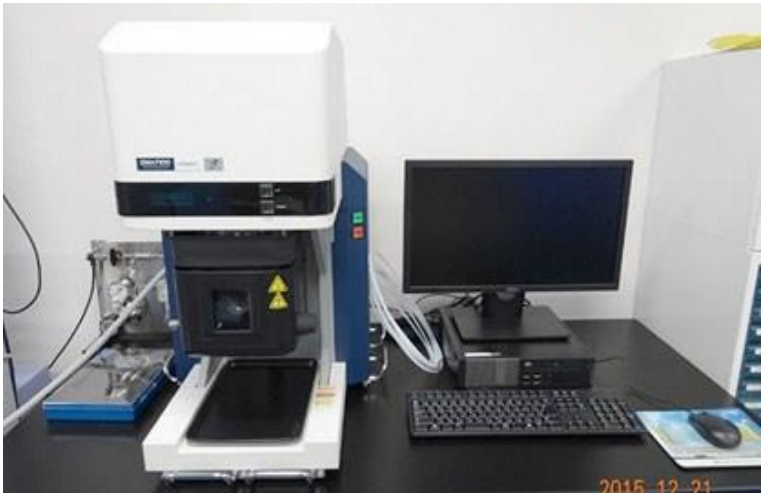

Figure 3-4 DMA Hitachi 7100

Figure 3-5 and 3-6 shows the plot for Young's Modulus of Solder and PCB. The plots have been made over a range of 0 to 150 deg C.

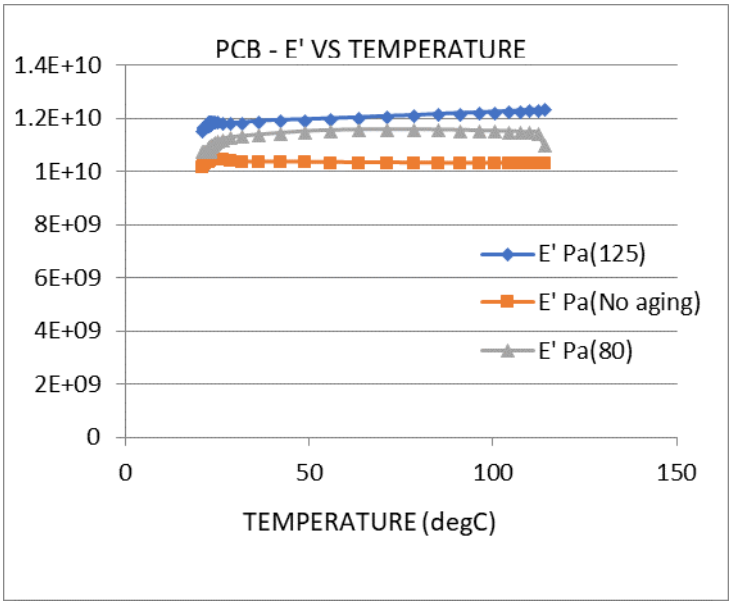

Figure 3-5 DMA plots for PCB

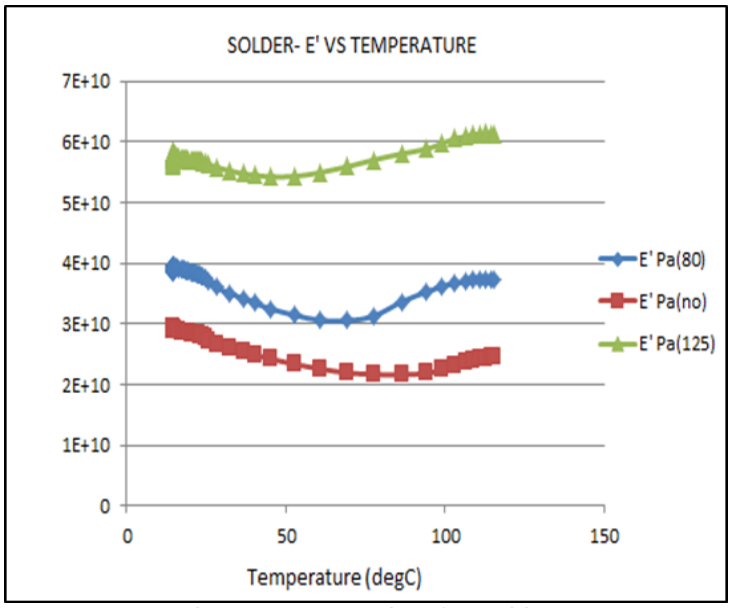

Figure 3-6 DMA plots for Solder

Material	Young's Modulus (Gpa)
Copper Pad	110
Die Attach	154
Die	150
Mold	24
Polyimide Layer	3.3
Solder Mask	4.6

Table 3-3 Young's Modulus of Components

Material	YM No Aging	YM aging 80	YM aging 125
Board	10423179854	10998546143	11890821241
Solder	37882151491	37882151491	57586777525

Table 3-4 Young's Modulus Average from the plots.

3.3 Temperature Chamber

The temperature chamber is used to expose the package to aggravated temperatures known as isothermal aging. The chamber has a 12"x4" borosilicate glass at the top wall for the cameras to view the package clearly. The purpose of using a borosilicate glass is to avoid any reflection caused due to illumination from glass surface into the camera eye.

There are two openings on each side wall of the oven which are covered by rubber corks. Thermocouple wires are connected to the sample through these openings which are closed with the rubber corks after the wires have been carefully passed through them. The package was exposed to temperatures of 80^{o}C and 125^{o}C for 3 and 5 days respectively.

Figure 3-7 Temperature Chamber

3.4 X-Ray Spectroscopy

When an electron from the inner shell of an atom is excited by the energy of a photon, it moves to a higher energy level. When it returns to the low energy level, the energy which it previously gained by the excitation is emitted as an electron which has a wavelength that is characteristic for the element (there could be several characteristic wavelengths per element). Analysis of the X-ray emission spectrum produces qualitative results about the elemental composition of the specimen. Comparison of the specimen's spectrum with the spectra of samples of known composition produces quantitative results (after some

mathematical corrections for absorption, fluorescence and atomic number). Atoms can be excited by a high-energy beam of charged particles such as electrons (in an electron microscope for example), protons (see PIXE) or a beam of X-rays (see X-ray fluorescence, or XRF). These methods enable elements from the entire periodic table to be analyzed, except for H, He and Li. In electron microscopy an electron beam excites X-rays; there are two main techniques for analysis of spectra of characteristic X-ray radiation: energy-dispersive X-ray spectroscopy (EDS) and wavelength dispersive X-ray spectroscopy (WDS).

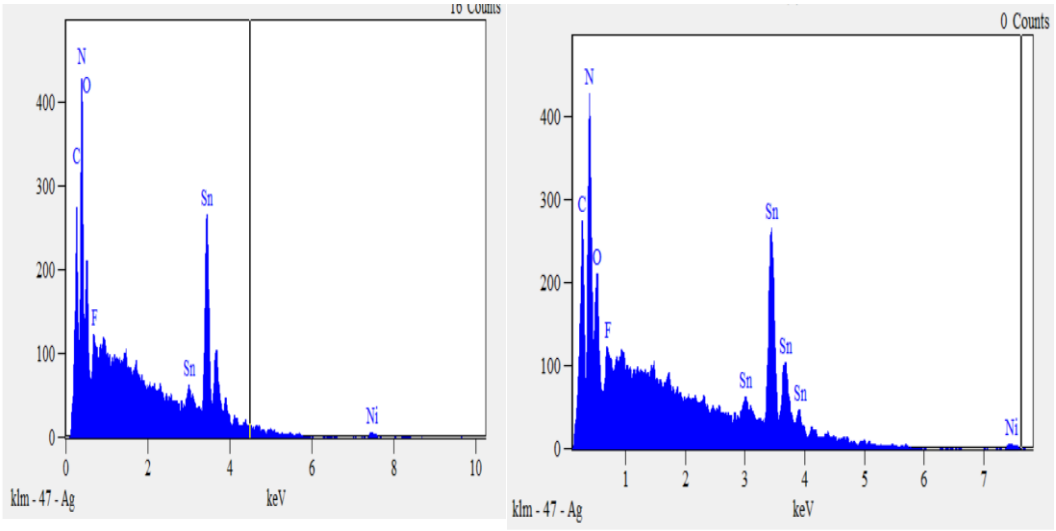

Quantitative Results for: Base(8)

Element Line	Net Counts	ZAF	Weight %	Norm. Wt.%	Atom %
C K	2605	1.583	19.18	19.18	31.41
N K	1960	2.864	25.60	25.60	35.96
O K	1447	5.782	18.60	18.60	22.87
F K	277	5.609	3.80	3.80	3.93
Ni K	139	1.169	2.31	2.31	0.77
Sn L	5370	1.294	30.52	30.52	5.06
Total			100.00	100.00	100.00

Quantitative Results for: Base(8)

Element Line	Net Counts	ZAF	Weight %	Norm. Wt.%	Atom %
C K	2605	1.583	19.18	19.18	31.41
N K	1960	2.864	25.60	25.60	35.96
O K	1447	5.782	18.60	18.60	22.87
F K	277	5.609	3.80	3.80	3.93
Ni K	139	1.169	2.31	2.31	0.77
Sn L	5370	1.294	30.52	30.52	5.06
Total			100.00	100.00	100.00

Figure 3-8 Results of X-Ray Spectroscopy

CHAPTER 4 FINITE ELEMENT MODELLING

Among the various numerical methods, Finite element method is the most popular and widely used method. Other than this it is considered as the most sophisticated tool for solving engineering problems. In this method, the whole continuum is divided into a finite number of elements of geometrically simple shape. These elements are made of several nodes. The unknown are the displacements of these nodes. To describe the unknown displacements at each point a polynomial interpolation function is used. The entire force applied to the structure is replaced by an equivalent system of forces applied to the nodes. [33] The result of the entire displacement of the structure is obtained by assembling the governing equation

$$\{F\} = [K]\{u\}, \text{ where}$$

$\{F\}$ = Nodal Load Vector

$[K]$ = Global Stiffness Matrix

$\{u\}$ = Nodal Displacements

4.1 APPLIACTIONS OF FEM IN ENGINEERING

- Aerospace/Mechanical/Civil/Automobile Engineering
- Structural Analysis(Static/Dynamic/Linear/Non-Linear)
- Thermal/Fluid flows
- Nuclear Engineering
- Electromagnetic
- Biomechanics
- Geomechanics
- Biomedical Engineering
- Hydraulics

4.2 STRUCTURAL ANALYSIS

To compute the deformations, internal forces and stress of a object, the structural analysis is used. To perform a structural analysis, we should first determine the structural loads, geometry, support conditions and material properties. This type of analysis can be used to capture the static response of the structure.

Example: Computation of deformations, internal forces, stresses and strains. The following are the areas in which structural analysis play a major role,

Static Analysis – Under static loading conditions, determining the displacements and stresses.

Modal Analysis – For determining the mode shapes and natural frequencies of a structure.

Harmonic Analysis – Under time varying loads, determining the harmonic response of the structure.

Transient Dynamic Analysis – Under random time varying loads, determining the response of the structure.

Spectrum Analysis – Due to a response spectrum or a random vibration input, calculating the stresses and strain of the structure.

Buckling Analysis – For calculating the buckling loads and determining the buckling load shape.

Advance Structural Analysis – This examines the dynamic response, stability and non-linear behavior of the structure.

Linear Static Analysis - In most of the analysis when assumptions like small deformation, perfectly elastic material and loads are assumed to be static, the analysis can be treated as a specific linear problem.

4.3 THERMAL ANALYSIS

In a thermal analysis we will be able to calculate the temperature gradients, heat transfer and thermal flux of an object. Three modes like conduction, convection and radiation analysis can be performed on the desired model. The thermal analysis can be performed in two areas:

• Steady State Thermal Analysis – Under static loading conditions they are used to determine the temperature gradient and other thermal quantities.

• Transient Thermal Analysis – Under time varying loading conditions, they are used to determine the temperature gradient and other thermal quantities.

4.4 STEPS IN FEM

There are several steps to complete an analysis by finite element method. These methods are in coincidence with the matrix method. The theoretical approach is given to each step below,

4.4.1 Discretization

Initially to start with, the problem must be divided into several elements, connect with nodes. This process is called discretization. Each element and their corresponding node should be numbered so that matrix of connectivity can be set up. The orders in which the nodes and elements are numbered are more important because it greatly affects the computation time. The reason is because we get a symmetrical, banded stiffness matrix, whose bandwidth is dependent on the difference in the node numbers for each element, and this bandwidth is in turn connected to the number of calculations that has to be done in the computer to solve the problem. Usually FEM programs perform an 26 internal numbering option to optimize this bandwidth to a minimum by renumbering these nodes if they are not optimal.

4.4.2 Element Analysis

To perform the element analysis there are two key components, one is expressing the displacements with in the elements and maintaining the equilibrium of the elements. Additionally, the stress-strain relationship should be maintaining compatibility. The result we obtain is the element stiffness relationship S=kv. These results could be obtained from the governing differential equation and boundary condition of the elements. For plane stress problems, the displacement within the elements are expressed as shape functions scaled by the node displacements. The displacement in an arbitrary point within the element is calculated by the nodal point displacement by assuming expression for shape functions. The section of the structure, which is made up of number of elements by which it is represented is kept by the stresses along the edges. Usually in finite element analysis it is easy to work with nodal point forces. The stress acting in the edge of the structure is replaced by the equivalent nodal point forces by making the element to be in an integrated equilibrium using work or energy considerations. This method of replacement is often called lump the edge forces to nodal forces. Thus, the relationship between the nodal point displacements and forces are expressed as S= kv + So where,

- S – Generalized nodal point forces
- K – Element stiffness matrix
- V – Nodal point displacements
- S^0 – Nodal point forces for external loads

4.4.3 System Analysis

A relationship between the load and nodal point displacements is established by demanding the equilibrium for all nodal points in the structure:

$$R = kr + R^0$$

By adding the contributions from the element stiffness matrices, we can establish the global stiffness matrix. Similarly, the load vector R is obtained from the known nodal forces.

4.4.4 Boundary Conditions

Boundary conditions are given to the structure by setting nodal displacements to known values of spring stiffness are added.

4.4.5 Finding Global Displacements

By solving the linear set of equations, we can calculate the global displacements,

$$r = K\text{-}1\ (R - R^0)$$

4.4.6 Calculation of Stresses

From Hooke's law, the stresses can be determined by the strains. Strains are in turn derived from the displacement functions within the element combined with Hooke's law. This can be expressed as,

$$\sigma\ (x, y, z) = D\ B(x, y, z)\ v$$

Where,

$v = a\ r$

D - Hooke's law on matrix form

B - Derived from u(x, y, z)

Finally, the post processors help users to sort the output and display it in the graphical form.

4.5 SUBMODELLING

In finite element analysis, the mesh developed in the element is too coarse to produce satisfactory results. Therefore, a method called submodelling is introduced to generate finer meshes in the specific region of interest.

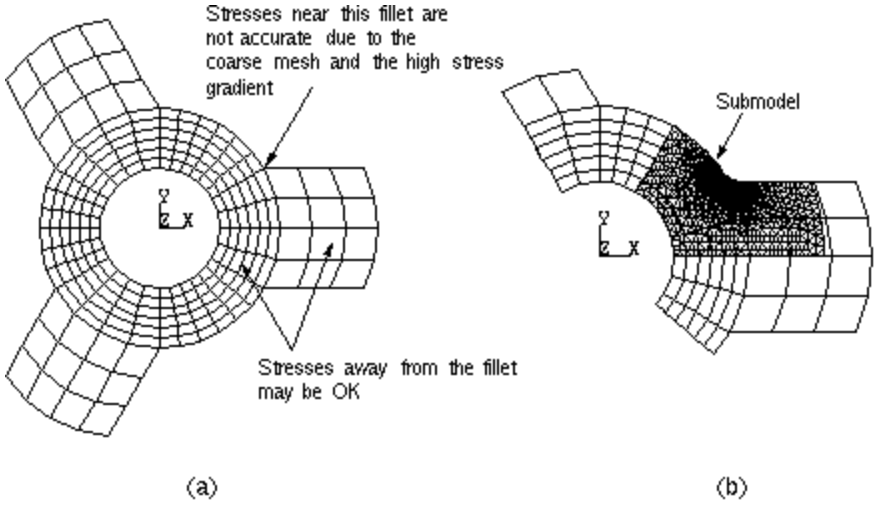

Figure 4-1 Sub-modelling method: (a) Coarsely Meshed model (b) Meshed Sub-model

Sub modeling is commonly known as cut boundary displacement method or the specified boundary displacement method. The cut boundary is the boundary of the sub model which represents a cut through the coarse model. Displacements calculated on the cut boundary of the coarse model are specified as boundary conditions for the sub model.

Sub modeling is based on St. Venant's principle, which states that if an actual distribution of forces is replaced by a statically equivalent system, the distribution of stress and strain is altered only near the regions of load application. The principle implies that stress concentration effects are localized around the concentration; therefore, if the boundaries of the sub model are far enough away from the stress concentration, reasonably accurate results can be calculated in the sub model.

The ANSYS program does not restrict sub modeling to structural (stress) analyses only. Sub modeling can be used effectively in other disciplines as well. For example, in a magnetic field analysis, you can use sub modeling to calculate more accurate magnetic forces in a region of interest.

Aside from the obvious benefit of giving you more accurate results in a region of your model, the sub modeling technique has other advantages:

o It reduces, or even eliminates, the need for complicated transition regions in solid finite element models.

o It enables you to experiment with different designs for the region of interest (different fillet radii, for example).

o It helps you in demonstrating the adequacy of mesh refinements.

Some restrictions for the use of sub modeling are:

o It is valid only for solid elements and shell elements.

o the principle behind sub modeling assumes that the cut boundaries are far enough away from the stress concentration region. You must verify that this assumption is adequately satisfied."

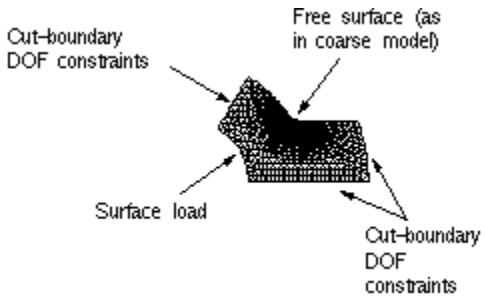

Figure 4-2 Sub-modelling Fundamentals

CHAPTER 5

MODELLING, METHODOLOGY AND SIMULATION

In this chapter Finite Element modeling, methodology and simulation which has been carried out to analyze the effect of thermal aging on crack growth behavior in lead free solder interconnects, on the overall reliability of the package, has been discussed in detail. It consists of the following steps:

- Processing subdivided into 3 steps
    1. Modelling the geometry.
    2. Assigning the material properties.
    3. Mesh Generation
- Solution subdivided into 4 sub steps
    1. Application of loads and boundary condition.
    2. Selection of output and load step controls.
    3. Selection of solver.
    4. Obtaining the solution.
- Post Processing
    1. Review the results obtained.

The following assumptions have been made while performing this FE analysis:

- The PCB is considered to be orthotropic.
- All materials except the solder balls are considered as linearly elastic.
- The solder is modeled as rate dependent viscoplastic material using Anand's Viscoplastic model.
- All parts in the package are assumed to be bonded to each other.

5.1 GEOMETRY

A silicon die, which is enclosed in a mold is attached to the substrate solder mask using a die attach. The substrate solder mask is further attached to the polyimide layer. The package has copper pads on both top and bottom sides of the solder balls. The cross-section of the BGA package modelled in this study is shown in the figure 5-1.

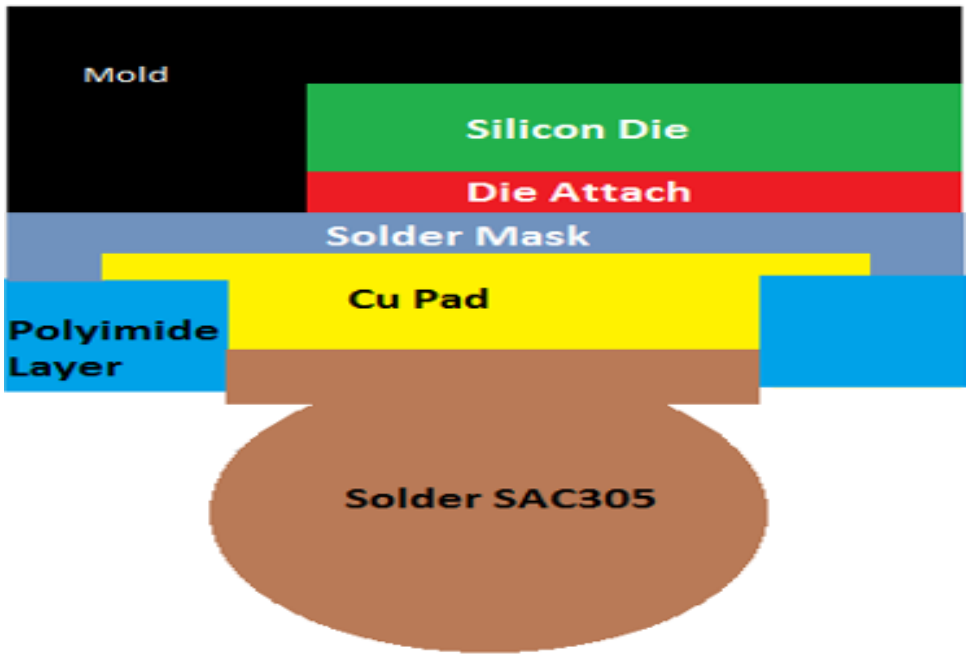

Figure 5-1 Detailed Drawing of a BGA package

Table 5-1 provides in detail the package components and their respective dimensions while fig 5-2 shows the schematic diagram of an BGA package. The FR-4 board used in the study has 8 layers (1-6-1) of copper. A 11 X 11 array Micro star BGA is modeled in ANSYS 18.

Component	Dimensions(mm)
Package	6 x 6 x 0.74
Die	4.5 x 4.5 x 0.28
Solder Ball Pitch	0.5
Solder Ball Diameter	0.3
Solder Ball Height	0.2
Solder Mask Thickness	0.05
Substrate Thickness	0.05
Copper Pad Thickness	0.04

Table 5-1 Package Detailed Dimensions

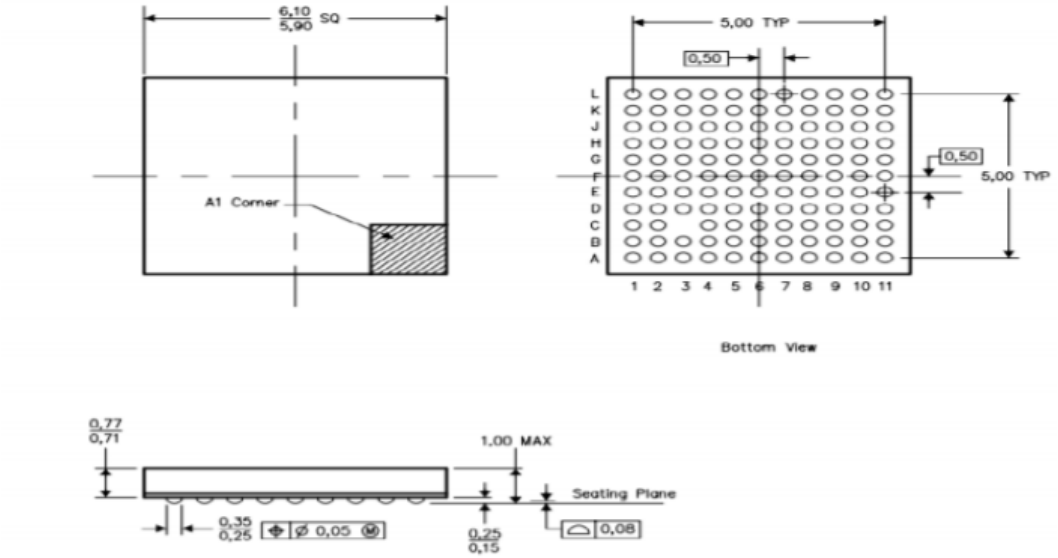

Figure 5-2 Schematic Diagram of BGA

A sub-model derived from global model is considered for the analysis. Figure 5-3 shows

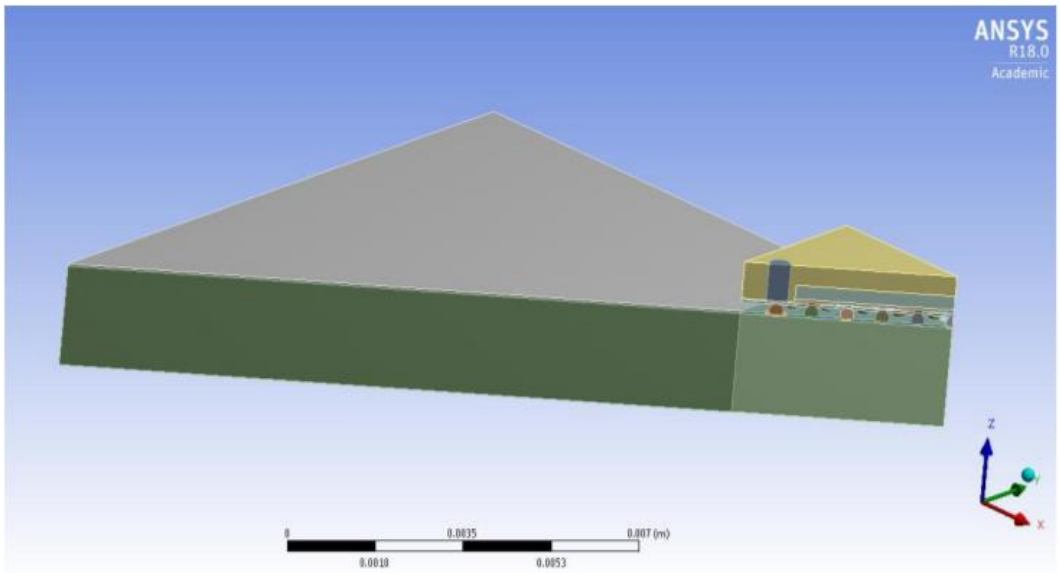

Figure 5-3 Octant Symmetry Model

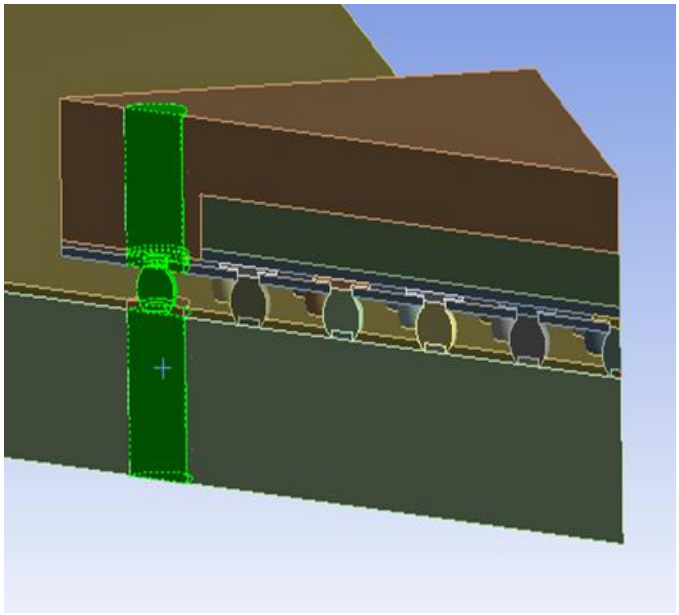
Figure 5-4 Octant Symmetry Model Highlighting the Sub model

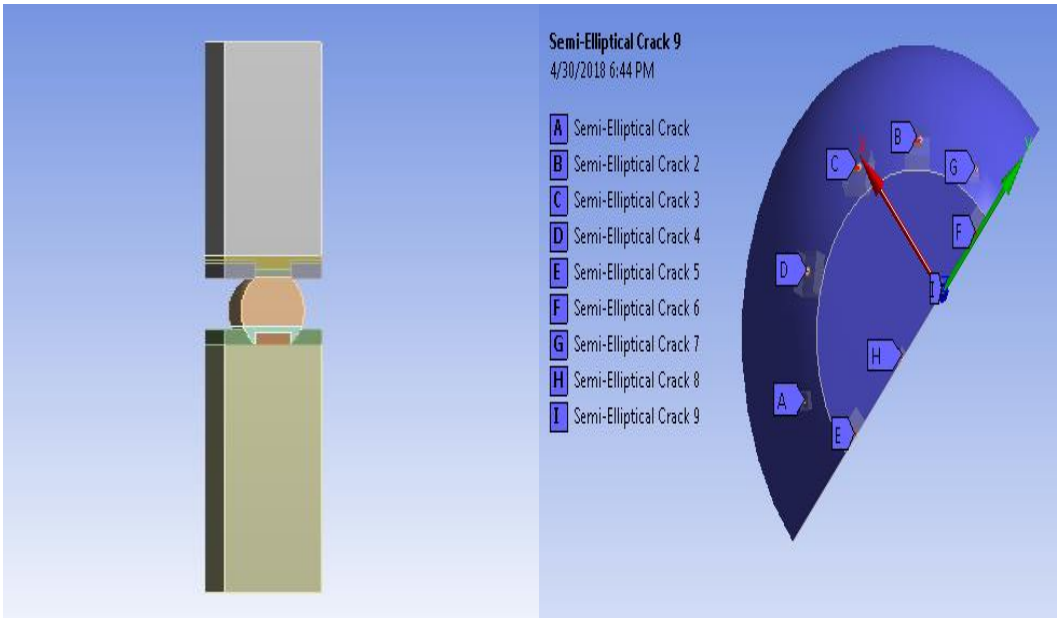

Figure 5-4 Exploded Sub-Model with Crack modelled locations

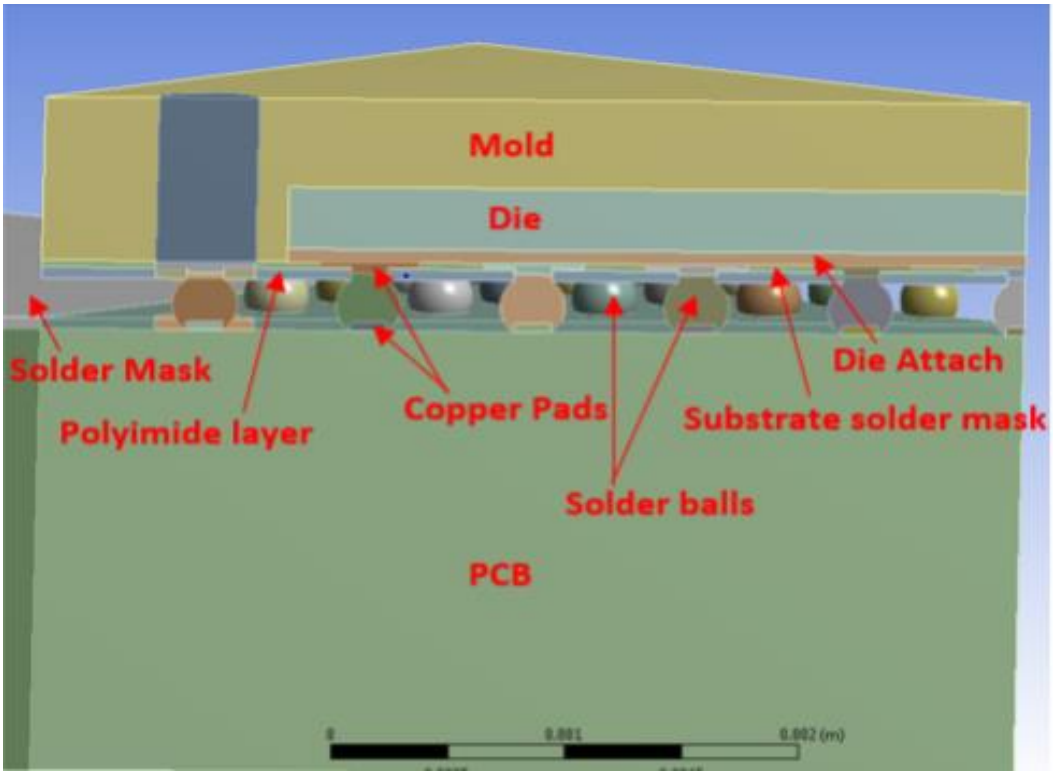

Figure 5-5 Cross-section of geometry

5.2 MATERIAL PROPERTIES

As already mentioned in the assumptions, the package is considered linearly elastic, PCB is orthotropic, and the solder ball is a rate dependent viscoplastic material modeled based on Anand's 18 viscoplastic law. The material properties determined during the material characterization are used. The input is given for the temperature dependent CTE, Young's modulus, Poisson's ratio and temperature dependent shear modulus. The solder all used is SAC305 whose composition is 96.5% Tin(Sn), 3% Silver(Ag) and 0.5% Copper(Cu). Using Anand's viscoplastic model both plastic deformation and creep are considered to represent the secondary creep of the solder.

The total strain is given by:

$$\epsilon_{ij} = \epsilon^{e}_{ij} + \epsilon_{ij}^{in}$$

Where $\epsilon ij\ in$ is the inelastic strain tensor.

Anand's viscoplastic model, the inelastic strain rate is coupled to the rate of deformation resistance.

Below equation gives the strain rate:

$$\frac{d\varepsilon_{in}}{dt} = A\left[\sin h\ \left(\xi\ \frac{\sigma}{s}\right)\right]^{\frac{1}{m}} \exp\left(-\frac{Q}{RT}\right)$$

The rate deformation resistance is given by:

$$\dot{s} = \left\{h_0(|B|)^{\alpha}\ \frac{B}{|B|}\right\} \frac{d\varepsilon_p}{dt}$$

$$B = 1 - \frac{s}{s^*}$$

$$s^* = \hat{s}\left[\frac{1}{A}\ \frac{d\varepsilon_p}{dt} \exp\left(-\frac{Q}{RT}\right)\right]$$

Where $\mathbb{d}\epsilon in\ \mathbb{d}t$ is the effective inelastic strain rate, σ is the effective true stress, s is the deformation resistance, T is the absolute temperature, A is pre-exponential factor, ξ is stress multiplier, m is the strain rate sensitivity of stress, Q is activation energy, R is universal gas constant, h0 is hardening/softening constant, ŝ is coefficient for deformation resistance saturation value, n is strain-rate sensitivity of saturation value, and a is strain rate sensitivity of hardening or softening. The nine material constants of Anand's viscoplastic law are listed in the table 5-2.

Constant	Name	Unit	Value
s0	Initial Deformation Resistance	MPa	12.41
Q/R	Activation Energy/ Universal Gas Constant	1/K	9400
A	Pre-exponential Factor	Sec^{-1}	4E+06
ξ	Multiplier of stress	Dimensionless	1.5
m	Strain Rate Sensitivity of Stress	Dimensionless	0.303
h0	Hardening Softening constant	Mpa	1378.8
$\hat{s}$	Co-efficient of deformation resistance Saturation	Mpa	0.07
n	Strain Rate Sensitivity of Saturation	Dimensionless	1.3
a	Strain Rate of Sensitivity of Hardening or Softening	Dimensionless	1.6832

Table 5-2 Anand's Constant for SAC 305

5.3 MESHING

Hex dominant meshing is used for the model except tetrahedron meshing for the solder ball due to semi-elliptical cracks being modelled on it. The critical solder is determined to the farthest from neutral point (midpoint of the package). Figure 5-6 below shows the meshing of the exploded sub model used for analysis. Statistics of the exploded sub-model suggest that there are 934544 nodes and 4488799 elements.

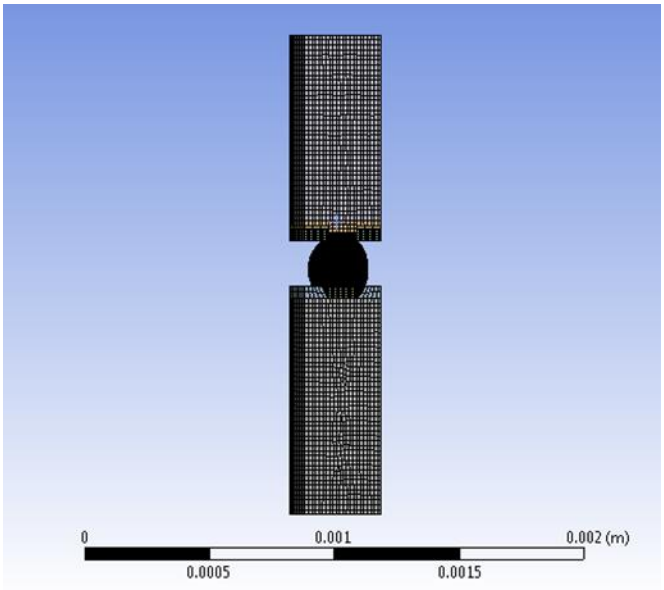

Figure 5-6 Meshing of Exploded Sub-model

5.4 LOADING ND BOUNDARY CONDITIONS

Loading and Boundary condition are the pillars of FE analysis. Loading and boundary conditions should be accurate to simulate realistic results. The package was tested for loading condition of Thermal Cycling. Symmetric boundary condition was taken for octant symmetry faces and the symmetric faces were given friction less support the common vertex was fixed (0 DOF). As for the sub model only frictionless support is given.

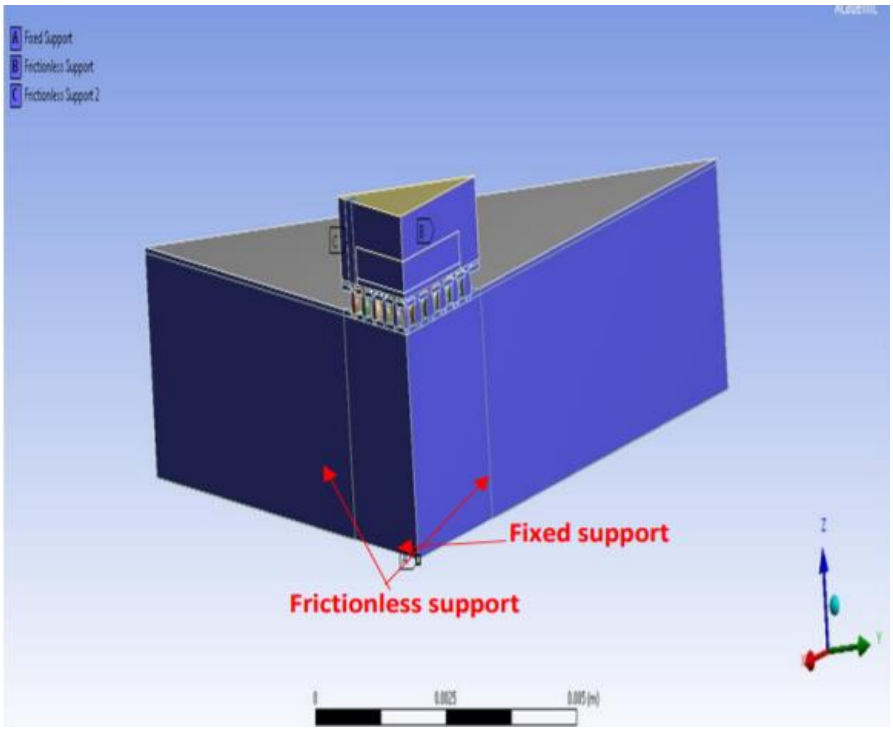

Figure 5-7 Boundary Conditions Ansys 18.0

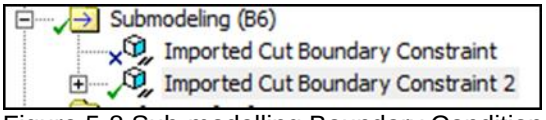

Figure 5-8 Sub-modelling Boundary Condition

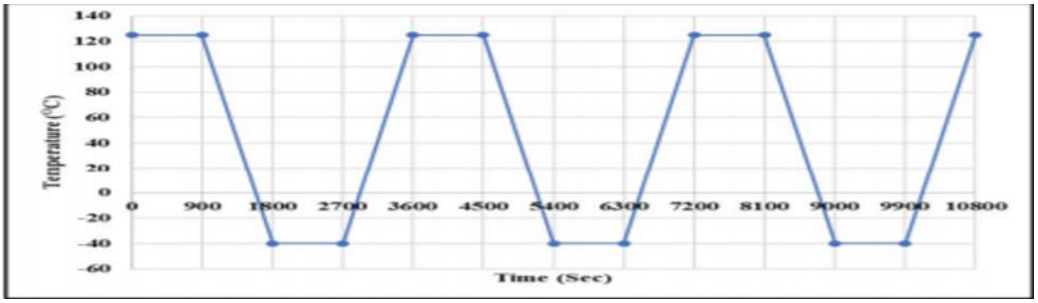

Figure 5-8 Thermal Cycling Profile

5.5 SEMI-ELLIPTICAL CRACK

Three types of cracks can be modelled in ANSYS 18.0. They are: pre-meshed, semi-elliptical and arbitrary crack. Sem-elliptical crack is chosen out of the three because it is the best representation of theoretical fracture out of the three. Fig 5-9 shows the detailed figure of a semi-elliptical crack and crack locations on the solder interconnects.

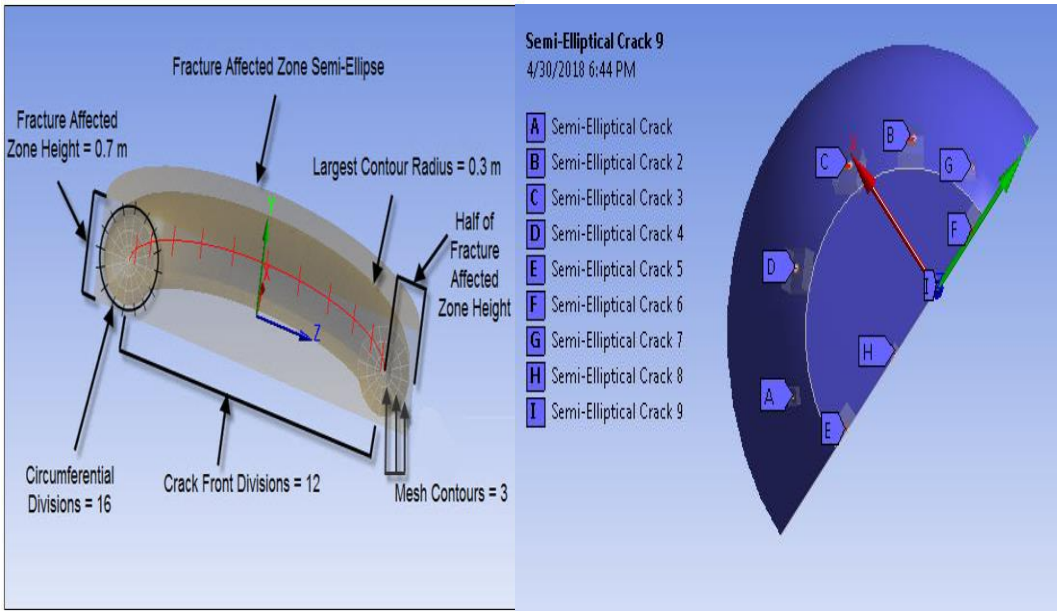

Figure 5-9 Semi-elliptical Crack Fundamentals

The crack locations were specifically chosen when the package was only exposed to thermal cycling. From the results of this model points of max elastic stain, normal and shear elastic strain, normal stress, max principle stress, principle elastic strain is found and cracks E, A, F, G, B are specifically modelled at these points. This is done to find out which of these stresses or strains can be critical to the reliability of the solder interconnects. The other cracks i.e. C, D, I are randomly modelled.

CHAPTER 6

RESULTS AND DISCUSSION

6.1 RESULTS

Fracture analysis of solder interconnects during thermal cycling after the components have been thermally aged process has been completed in ANSYS Workbench v18.0. The aim of this study was to identify the critical crack, its location and mode of failure so that area of interest can be found out near which if cracks are developed would lead to failure of solder interconnects, saving experimenting cost and time. J-integral, SIF values have been found out for each crack and compared to show the severity of cracks in a particular region. Finally, plastic work for all the three models and their respective cycles to failure have been found to show prove that isothermal aging has a deleterious effect on the life of the package.

6.1.1 J-integral(J/m^2) Results:

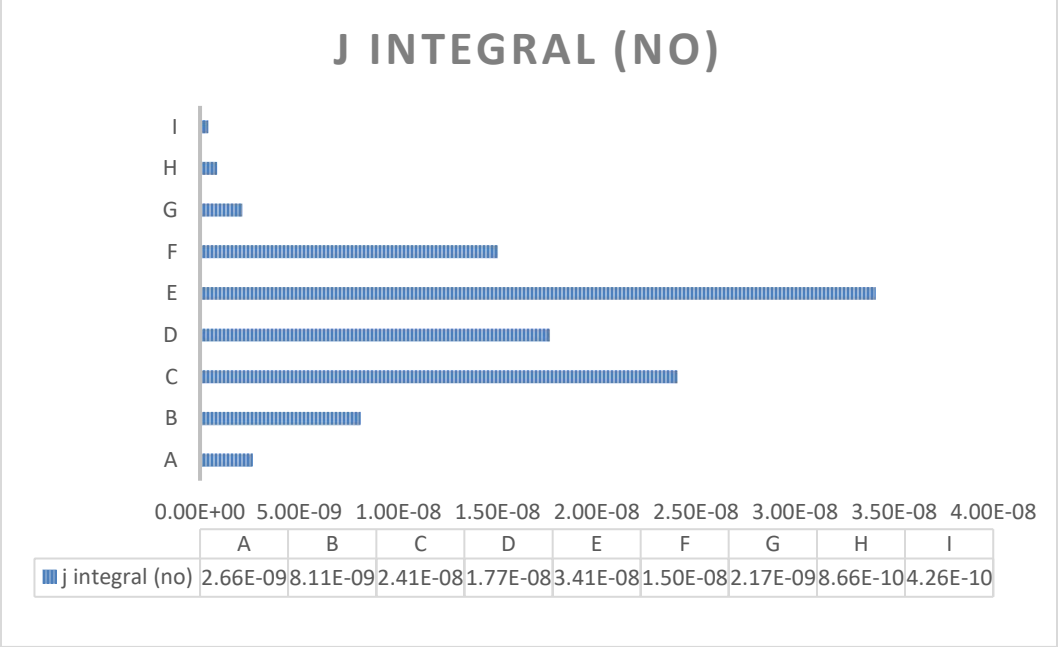

	A	B	C	D	E	F	G	H	I
j integral (no)	2.66E-09	8.11E-09	2.41E-08	1.77E-08	3.41E-08	1.50E-08	2.17E-09	8.66E-10	4.26E-10

Figure 6-1 J-int for No aging Model

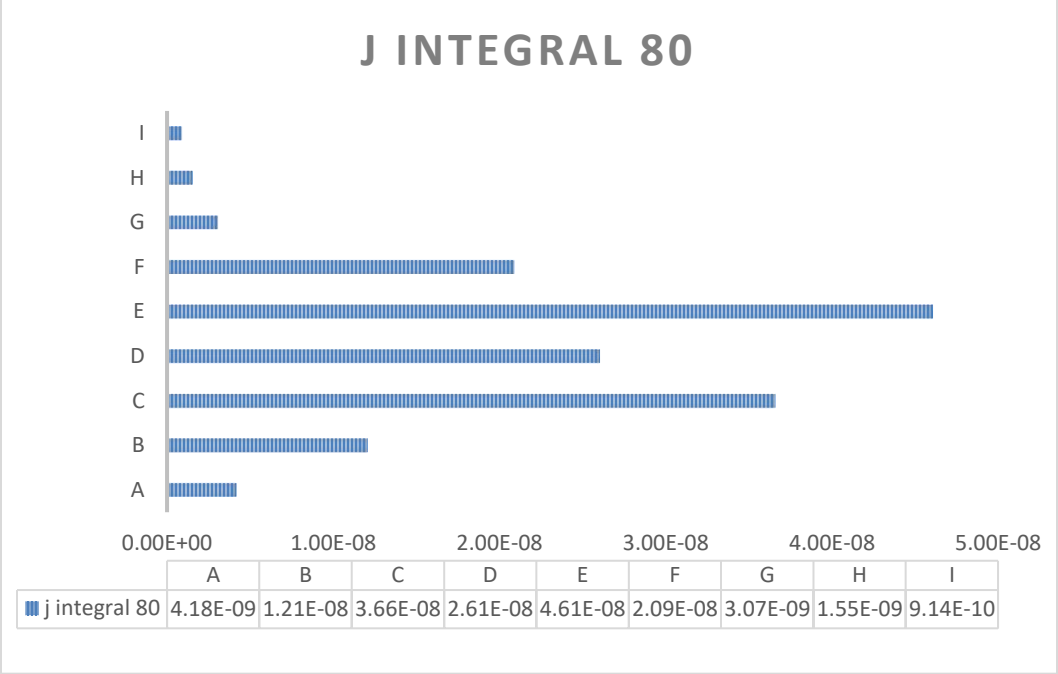

	A	B	C	D	E	F	G	H	I
j integral 80	4.18E-09	1.21E-08	3.66E-08	2.61E-08	4.61E-08	2.09E-08	3.07E-09	1.55E-09	9.14E-10

Figure 6-2 J-int for 80degC aged Model

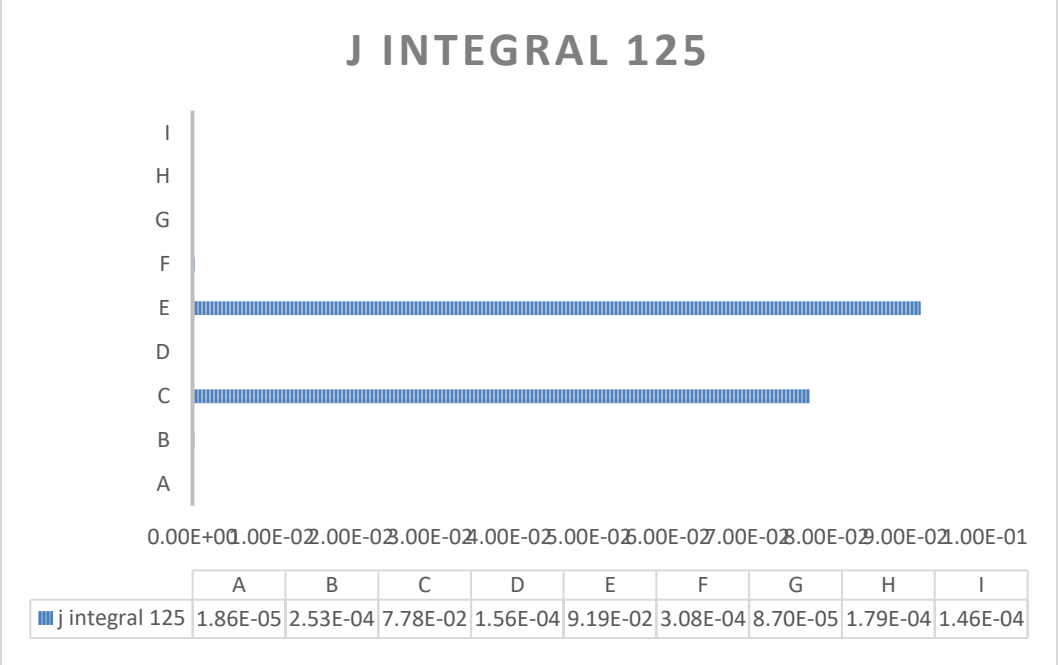

	A	B	C	D	E	F	G	H	I
j integral 125	1.86E-05	2.53E-04	7.78E-02	1.56E-04	9.19E-02	3.08E-04	8.70E-05	1.79E-04	1.46E-04

Figure 6-3 J-int for 125degC aged Model

6.1.2 Stress Intensity Factor (SIF)(Pa*m$^{0.5}$) Results:

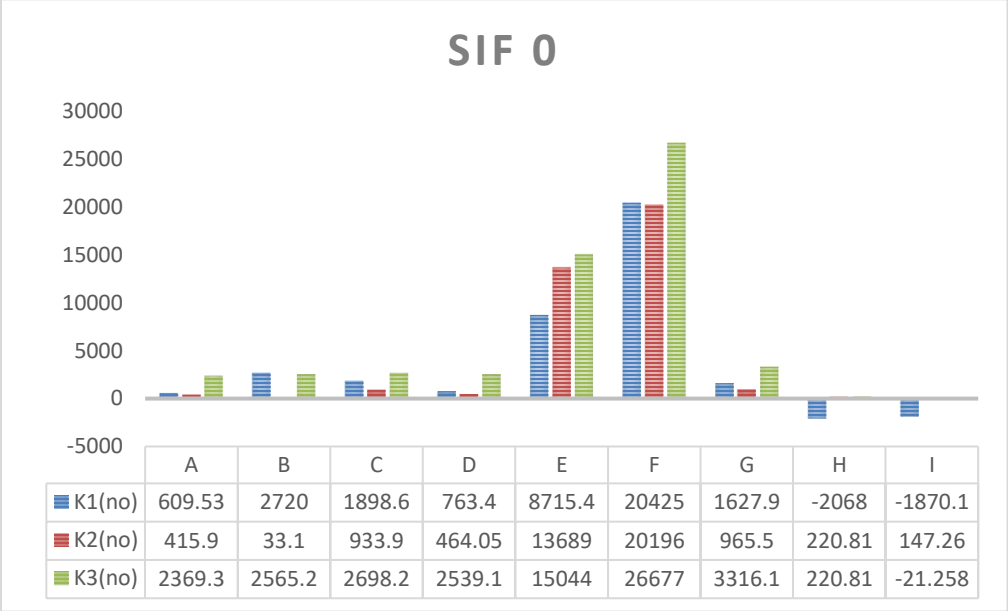

	A	B	C	D	E	F	G	H	I
K1(no)	609.53	2720	1898.6	763.4	8715.4	20425	1627.9	-2068	-1870.1
K2(no)	415.9	33.1	933.9	464.05	13689	20196	965.5	220.81	147.26
K3(no)	2369.3	2565.2	2698.2	2539.1	15044	26677	3316.1	220.81	-21.258

Figure 6-4 SIF for No aging Model

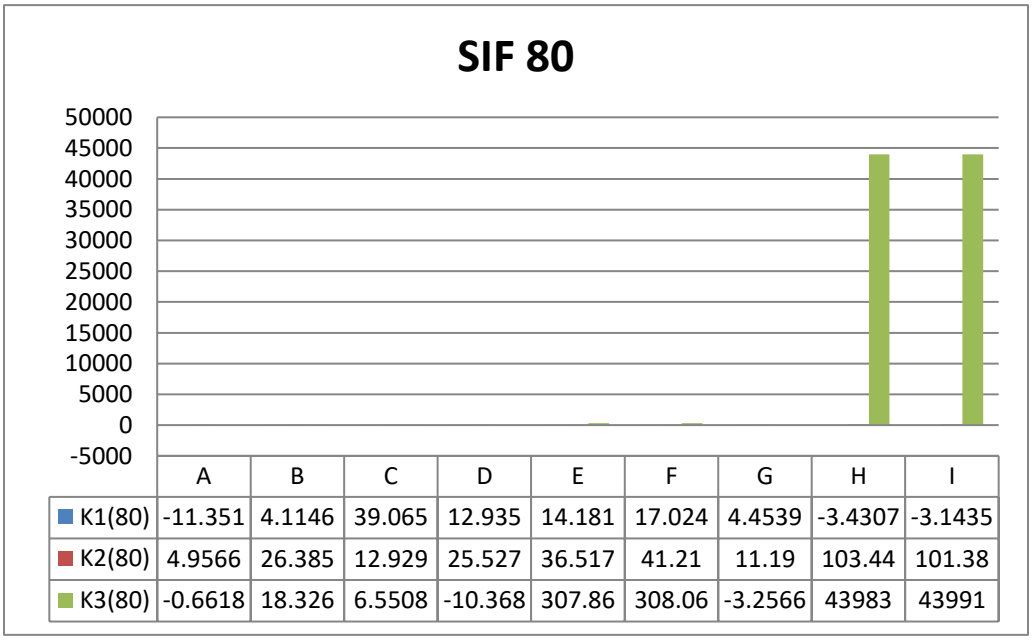

	A	B	C	D	E	F	G	H	I
K1(80)	-11.351	4.1146	39.065	12.935	14.181	17.024	4.4539	-3.4307	-3.1435
K2(80)	4.9566	26.385	12.929	25.527	36.517	41.21	11.19	103.44	101.38
K3(80)	-0.6618	18.326	6.5508	-10.368	307.86	308.06	-3.2566	43983	43991

Figure 6-5 SIF for 80degC aged Model

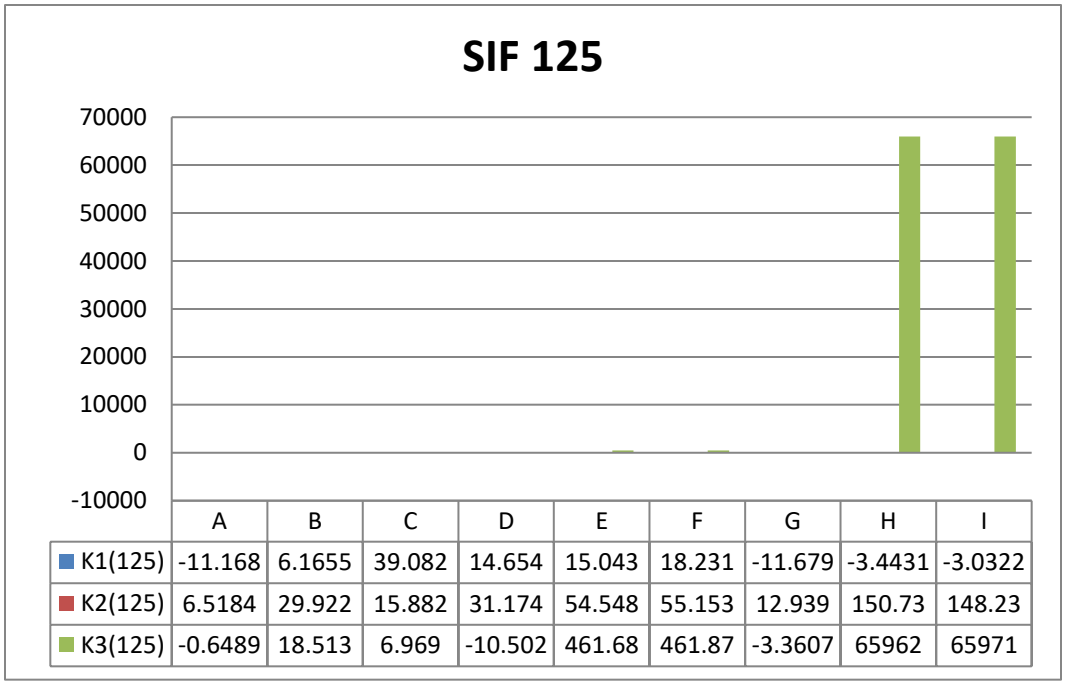

	A	B	C	D	E	F	G	H	I
K1(125)	-11.168	6.1655	39.082	14.654	15.043	18.231	-11.679	-3.4431	-3.0322
K2(125)	6.5184	29.922	15.882	31.174	54.548	55.153	12.939	150.73	148.23
K3(125)	-0.6489	18.513	6.969	-10.502	461.68	461.87	-3.3607	65962	65971

Figure 6-6 SIF for 125degC aged Model

From the above values for SIF it should be noted that negative value of SIF means the crack will propagate under compressive load. Furthermore, if the SIF i.e. K is less than K_c i.e. fracture toughness, crack propagation would not take place.

6.1.3 Plastic Work

Below is the APDL code that is used to calculate plastic work on the critical solder ball, in turn suggesting which model will fail first.

!APDL SCRIPT TO CALCULATE PLASTIC WORK

/post1

allsel,all

!CALC AVG PLASTIC WORK FOR CYCLE1

set,4,last,1 !LOAD STEP

cmsel,s,Critical,elem !ELEMENT FOR VOL AVERGAING

etable,vo1table,volu

pretab,vo1table

etable,vse1table,nl,plwk !PLASTIC WORK

pretab,vse1table

smult,pw1table,vo1table,vse1table

ssum

**get,splwk,ssum,,item,pw1table*

**get,svolu,ssum,,item,vo1table*

pw1=splwk/svolu !AVERAGE PLASTIC WORK

!CALC AVG PLASTIC WORK FOR CYCLE2

set,8,last,1 !LOAD STEP

cmsel,s,Critical,elem

etable,vo2table,volu

pretab,vo2table

etable,vse2table,nl,plwk !PLASTIC WORK

pretab,vse2table

smult,pw2table,vo2table,vse2table

ssum

**get,splwk,ssum,,item,pw2table*

**get,svolu,ssum,,item,vo2table*

pw2=splwk/svolu !AVERAGE PLASTIC WORK

!CALC DELTA AVG PLASTIC WORK

pwa=pw2-pw1

!CALC AVG PLASTIC WORK FOR CYCLE3

set,12,last,1 !LOAD STEP

cmsel,s,Critical,elem

etable,vo3table,volu

pretab,vo3table

etable,vse3table,nl,plwk !PLASTIC WORK

pretab,vse3table

smult,pw3table,vo3table,vse3table

ssum

**get,splwk,ssum,,item,pw3table*

**get,svolu,ssum,,item,vo3table*

pw3=splwk/svolu !AVERAGE PLASTIC WORK

!CALC DELTA AVG PLASTIC WORK

pwb=pw3-pw2

my_pwb=pwb

my_pwa=pwa

my_pw1=pw1

my_pw2=pw2

my_pw3=pw3! Commands inserted into this file will be executed immediately after the ANSYS /POST1 command.

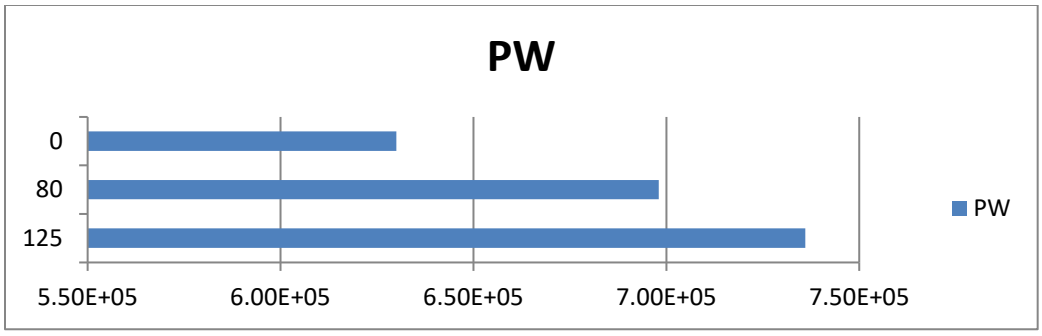

Figure 6-7 Plastic Work for All three Models

The above results suggest that plastic work is max for 125deC model and least for the no aging model.

6.1.4 Cycles to Failure

Volume averaged plastic work was calculated by writing an APDL script in the ANSYS commands using the stress and strain values from the FEA model. This volume averaged plastic work was related life cycles to failure using Syed's Model.

$$N_f = (A / \Delta W)^k$$

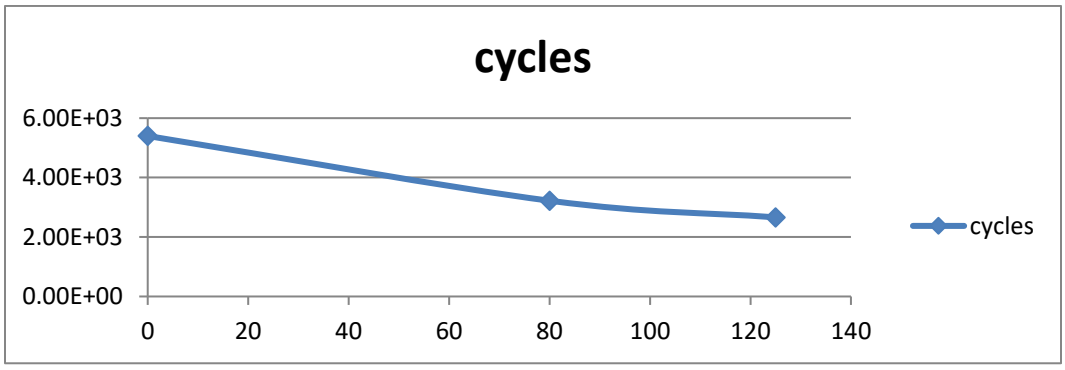

Figure 6-8 Plot for No. of cycles to Failure

6.2 CONCLUSION

A 3-D model for BGA Package has been formulated in ANSYS Workbench 18.0. Furthermore, the critical crack and its mode of failure has been found out. It was seen that thermal aging has a deleterious effect on the thermal cycling reliability of the package. The increase in aging temperature led to decrease in life of the package. Also, it was evident from the J-integral plots for all the three models that crack E had the maximum J-integral, therefore it is considered to be the critical crack. From SIF plots it can be seen that most of the cracks will fail by Mode 1 type i.e. opening. Crack E being the critical crack also suggests that cracks near the max elastic strain were more prone to failure than other areas. The second critical crack is C, this suggests that only max elastic strain should be taken into consideration while studying fracture in solder interconnects.

6.3 FUTURE WORK

- For the same work aging time and temperature can be increased to find the effects that would have on the crack growth and overall package.
- Crack growth study in other components of the package can studied. For e.g. PCB.
- Effects of thermal aging on drop test reliability of the BGA package can be studied.
- Study effects of aging at temperatures below 0 degC.

REFERENCES

[1] J. Zhang et al., "Thermal Aging Effects on the Thermal Cycling Reliability of Lead-Free Fine Pitch Packages," in IEEE Transactions on Components, Packaging and Manufacturing Technology, vol. 3, no. 8, pp. 1348-1357, Aug. 2013.

[2] M. Motalab et al., "Correlation of reliability models including aging effects with thermal cycling reliability data," 2013 IEEE 63rd Electronic Components and Technology Conference, Las Vegas, NV, 2013, pp. 986-1004.

[3] Luhua Xu, J. H. L. Pang, K. H. Prakash and T. H. Low, "Isothermal and thermal cycling aging on IMC growth rate in lead-free and lead-based solder interface," in IEEE Transactions on Components and Packaging Technologies, vol. 28, no. 3, pp. 408-414, Sept. 2005.

[4] Yang, Daoguo & Cui, Zaifu. (2011). The effect of thermal aging on the mechanical properties of molding compounds and the reliability of electronic packages. 1-4. 10.1109/ICEPT.2011.6067004.

[5] B. Rodgers, J. Punch and J. Jarvis, "Finite element modelling of a BGA package subjected to thermal and power cycling," ITherm 2002. Eighth Intersociety Conference on Thermal and Thermomechanical Phenomena in Electronic Systems (Cat. No.02CH37258), 2002, pp. 993-1000.

[6] J. H. Lau, "Solder joint reliability of flip chip and plastic ball grid array assemblies under thermal, mechanical, and vibrational conditions," in IEEE Transactions on Components, Packaging, and Manufacturing Technology: Part B, vol. 19, no. 4, pp. 728-735, Nov 1996.

[7] I. S. Raju, J. C. Newman jr “Stress-intensity factors for a wide range of semi-elliptical surface cracks in finite-thickness plates”, NASA-Langley Research Center, Hampton, Virginia, USA

[8] Begley, J. and Landes, J., "The J Integral as a Fracture Criterion," STP38816S Fracture Toughness: Part II, STP38816S, H. Corten, Ed., ASTM International, West Conshohocken, PA, 1972, pp. 1-23

[9] U. Rahangdale et al., "Damage progression study of 3D TSV package during reflow, thermal shocks and thermal cycling," 2017 16th IEEE Intersociety Conference on Thermal and Thermomechanical Phenomena in Electronic Systems (ITherm), Orlando, FL, 2017, pp. 1119-1125.

[10] Q. Yu, H. Kikuchi, S. Ikeda, M. Shiratori, M. Kakino and N. Fujiwara, "Dynamic behavior of electronics package and impact reliability of BGA solder joints," ITherm 2002. Eighth Intersociety Conference on Thermal and Thermomechanical Phenomena in Electronic Systems (Cat. No.02CH37258), 2002, pp. 953-960.

[11] T.H. Wang, Y.S. Lai, “Submodeling Analysis for Path-Dependent Thermomechanical Problems” Journal of ELECTRONICS PACKAGING, 2005